Edinburgh Research Explorer

Development of tissue engineered ligaments with titanium spring reinforcement

Development of tissue engineered ligaments with titanium spring reinforcement[†]

Anqi Wang,[a‡] Richard L. Williams,[∗a‡] Neeraj Jumbu,[a‡] Jennifer Z. Paxton,[b‡] Edward T. Davis,[c] Martyn A. Snow,[c] Alastair C. Ritchie,[d] Carina B. Johannson,[e] Rachel L. Sammons,[f] and Liam M. Grover[a]

Tissue engineering offers a promising alternative to the use of autografts in the treatment of ligament injuries. However, current approaches using only biodegradable materials have insufficient mechanical strength for load bearing applications. In this research, hybrid bio-artificial ligaments were fabricated using a combination of a titanium alloy spring and a fibrin gel/fibroblast construct. The ends of the ligament prosthesis were incorporated into brushite cement anchors to allow fusion with the host bone. Cell attachment to the titanium spring was examined using scanning electron microscopy and fluorescent staining of cells. The unreinforced constructs were observed to fail at the anchor-ligament junction, while the titanium spring reinforcement was found to assist in even transmission of the load to the ligament, and hence to provide a means of load sharing between the biological construct and the spring. As a result, the reinforced construct failed primarily in the soft tissue region. The good load distribution features from the mechanical data was attributed to the good cellular level adhesion to, and alignment along the coiling of, the length of the spring reinforcement. Incorporation of a biocompatible reinforcement in conjunction with a tissue engineered construct gave improved load distribution, reducing stress concentrations, and significantly increased the ultimate strength at failure. The results suggest that the hybrid approach used here shows promise in developing improved therapies for connective tissue injuries.

1 Introduction

Injuries to ligaments and tendons are common, and often are associated with poor rehabilitation outcomes due to the poor ability of these soft tissues for self-repair. The anterior cruciate ligament (ACL) of the knee joint, for example, has a high incidence of injury with recent studies reporting 8-37 ACL tears per 100,000[1,2]. The hard-soft tissue interface of the ACL consists of a hierarchically structured mineralised gradient extending from the bone and sweeping into the collagenous matrix of the ligament, which facilitates efficient force transduction while under strain and aids in maintaining overall joint stability. As an area of high stress concentration, the interface is frequently injured during sporting activities or by disease[3]. Tissue autografts, such as bone-patella and hamstring grafts, are the well-established gold standard treatment because they currently offer the most viable means of re-establishing the hard-soft interface as well as replacing the damaged soft tissue. However, this procedure often leads to pain, muscle weakness, instability and donor site morbidity[4,5]. As with many autograft-based treatment approaches, there is a finite amount of tissue available to harvest should the original graft fail.

The current challenge in tissue engineering is to reproduce the interface, which does not regenerate following graft therapy and is prone to failure post-surgery[6]. Tissue engineering approaches using only biodegradable materials show considerable promise but are limited currently by insufficient mechanical strength and inadequate fixation to the bones[7], both of which may lead to graft failure and consequent injury. A systematic review of synthetic ACL reconstruction[8] has concluded that while the latest tech-

∗ Corresponding author: Dr. Richard L. Williams, email: r.l.williams.2@bham.ac.uk

a School of Chemical Engineering, University of Birmingham, Edgbaston, Birmingham, B15 2TT, UK

b Centre for Integrative Physiology, Hugh Robson Building, The University of Edinburgh, 15 George Square, Edinburgh, EH8 9XD, UK

c The Royal Orthopaedic Hospital NHS Foundation Trust, Bristol Road South, Birmingham B31 2AP, UK

d Department of Mechanical, Materials and Manufacturing Engineering, University of Nottingham, Nottingham, NG7 2RD, UK

e Department of Prosthodontics, Institute of Odontology, The Sahlgrenska Academy, University of Gothenburg, P.O. Box 450, SE-405 30, Gothenburg, Sweden

f The School of Dentistry, College of Medical and Dental Sciences, University of Birmingham, St Chad's Queensway, Birmingham, B4 6NN, UK

† Electronic Supplementary Information (ESI) available: [details of any supplementary information available should be included here]. See DOI: 10.1039/b000000x/

‡ These authors contributed equally to this work.

niques have low failure rates and good clinical outcomes after 50 months, the technique remains less popular than the use of autografts, particularly with regard to joint stability. Tissue engineering approaches are still in their infancy, and constructs consisting of biodegradable and/or bioerodible scaffolds combined with autograft tissues or autograft cells are being investigated in animal models[7]. Composite or hybrid scaffolds that aim to improve scaffold mechanical properties and/or enhance cell adhesion and proliferation have been employed by several researchers[9–11]. Our group developed a method of producing bone-to-bone ligament construct *in vitro* using two brushite anchors and a cell-seeded fibrin gel, where the cell population causes contraction of the fibrin matrix to form a thin sinew-like construct running between the two anchors, containing highly aligned collagen in abundance[12,13]. Chemical supplementation of the culture media with TGF-β1, proline and ascorbic acid and intermittent mechanical stretching can all be used to accelerate contraction and significantly increase collagen content[12,14]. Ascorbic acid is an essential cofactor in procollagen chain hydroxylation and plays a key role in collagen fibrillogenesis[15–18], while proline is a major component of the collagen tri-peptide sequence[15,16]. Intermittent stretching of the construct during formation increases ERK1/2 phosphorylation and pro collagen mRNA[14]. The clinical concept involves implanting the constructs by fixating the brushite anchors into pilot holes drilled into the bone tissue. Brushite is almost entirely resorbed *in vivo* since it is one of the most soluble calcium orthophosphates in physiological conditions[19,20]. Previous work by our group has shown that the degradation profile can be prolonged by replacing the acidic orthophosphate ion in the cement reaction with a pyrophosphate ion, which inhibits the formation of the insoluble byproduct hydroxyapatite that is very difficult to resorb by the body[20]. Such formulations have been shown to permit high levels of bone ingression 6-12 months post implantation in a critical sized animal defect model[21]. In their current form, bone to bone ligament replacements cannot match the strength of the native tissue and therefore cannot be implanted in a fully load bearing situation.

In this research this shortcoming is addressed by reinforcing the construct with a titanium spring embedded in the fibrin matrix and fixed between the brushite anchors, that would then form the core of the construct as the matrix contracts over time. It was expected that incorporating a titanium spring into the soft tissue construct during formation will provide the initial support to allow rigorous loading regimes in culture to increase collagen deposition, thus increasing graft mechanical integrity prior to implantation, and additional support following implantation. Establishing a graft with sufficient long-term mechanical integrity to withstand daily motion and permit suitable post-surgical rehabilitation regimes will be of particular benefit to younger patients. The use of a synthetic reinforcement in conjunction with a tissue engineered construct offers resilience and improved mechanical properties in addition to improved load sharing between the reinforcement and the tissue engineered construct. A titanium spring was chosen as the reinforcement material in this study due to the well proven biocompatibility of titanium, the suitability of the spring constants of commercially available titanium springs,

and the ability of the springs to deform elastically without permanent deformation in the range of strains required. The effect of the spring construct formation, cell response and the mechanical properties was examined, leading to the production of a reinforced tissue-engineered ligament structure that has the potential to be implanted in a semi-load or load-bearing model.

2 Experimental Methods

2.1 Primary fibroblast extraction and culture

Embryonic chick tendon fibroblasts (CTFs) were isolated from day 13 chick embryos though digestion in a 2% type II collagense solution for 1 hr. CTFs were grown in Dulbecco's Modified Eagle's Medium (D6545, Sigma-Aldrich, Dorset, UK) supplemented with (v/v%) 10% Fetal Bovine Serum (A15-105 Mycoplex, PAA, Yeovil, UK), 1% penicillin streptomycin (P4333, Sigma-Aldrich, Dorset, UK), 1% HEPES (H0887, Sigma-Aldrich, Dorset, UK) and 2.4% L-glutamine (G7513, Sigma-Aldrich, Dorset, UK) - herein this supplemented culture media is referred to as "SDMEM". CTFs were used between passages 2 and 6.

2.2 Titanium substrates

Ti springs (TiS) with gaps of: 0 μm, 25 μm, 50 μm and 100 μm (Hi-Lex Corp. Ltd, Japan) were used initially in a screening process of their mechanical properties in order to decide on the best spring to use in the formation of reinforced ligament constructs. A table displaying the dimensions of the TiS used for preliminary mechanical testing is presented in Supplementary Information S2.2 Table S1. A titanium spring with a nominal coil gap of 100μm was selected as most suitable for the application as it allowed the largest cyclic load range. Titanium springs were placed in a cell suspension containing $1x10^4$ CTF cells/ml in multiwell plates in supplemented DMEM. Cell adhesion at day 5 or 6 and topography of Ti substrates was assessed using scanning electron microscopy (SEM) (JEOL JSM 840, Tokyo, Japan). To compare cell growth on different Ti specimens, the samples were fixed in 2.5% EM grade glutaraldehyde buffer (25% E.M. Grade, AGR1010, Agar Scientific, Essex, UK) in 0.1 M sodium cacodylate set to pH 7.3 (20840-25G-F, Sigma-Aldrich, Dorset, UK) for 10 min and dehydrated in an ethanol series from 20% to 100% for 10 min in each solution, using liquid CO_2 in a critical point drier (Polaron Critical Point Drier) as the final step. The samples were then coated with gold and examined using environmental SEM (FEI XL-30 environmental SEM, Oregon, USA).

2.3 Formation of tissue-engineered ligaments (TEL) with titanium spring (TiS) reinforcement

2.3.1 Manufacture of brushite anchors with embedded titanium springs.

Individual brushite anchors were prepared as described by Paxton *et al.*[22] (anchor shape (e)) to prepare control Tissue Engineered Ligaments (TEL) without Titanium Spring (TiS) reinforcement. A spring-cement skeleton for the Ti-reinforced TEL was prepared as shown in Supplementary Information, Section 2.3.1, Figure S1. First, wax models of the anchor were prepared (Figure

S1a), trimmed to 3mm in height and were manually pasted to the two ends of a 12mm long stainless steel wire (Figure S1b). This model, with the wire side facing down, was then pasted onto a plastic plate. The plate was filled with Elite double 22 resin (Zhermack, Badia Polesine, Italy) until the paste level rose to the top of the wax anchor (Figure S1c). The wax anchors and the wires were removed from the mould as soon as the resin was set, thus forming the mould for the spring-cement skeleton. A 15mm long TiS was placed where the stainless steel wire (12mm long) was previously positioned, with the two ends extending into the anchor position (Figure S1d). This mould was then placed on a flat resin mat (Figure S1e). The mould was filled with brushite cement paste manufactured by mixing β-Tricalcium phosphate powder with 3.5M Orthophosphoric acid at a powder to liquid ratio of 1g/ml. Before cement paste setting, an insect pin was secured through each cement anchor region into the resin mat (Figure S1f). The assembly was left at 37°C overnight and the cement-spring system was then removed from the mould (Figure S1g).

2.3.2 Formation of tissue-engineered ligaments (TEL).

The combined brushite anchor and titanium spring configuration described in section 2.3.1 was pinned onto the surface of a 35mm Petri dish coated with 2ml of Sylgard (Dow Corning, Midland, MI, USA). The anchors, spring and dish were sterilised in 70% ethanol for 20 min. Once sterile, 1ml growth medium supplemented with 10U/ml thrombin (605157, Merck Chemicals Ltd., Nottingham, UK), 2 μl/ml 200 mM aminohexanoic acid (07260-100G, Sigma-Aldrich, Dorset, UK) and 2μl/ml 10mg/ml aprotinin (10236624001, Roche Diagnostics Ltd., West Sussex UK) were added to the dish and agitated to cover the bottom. 400μl 20 mg/ml fibrinogen (F8630-1G, Sigma-Aldrich, Dorset, UK) was then added dropwise over the thrombin covered dish and incubated at 37°C for 1 hour to allow for fibrin polymerisation. Once the fibrin layer had formed 2ml of 1×10^5 CTF cells were seeded onto the fibrin gel. Note that these amounts are double that reported in previous studies by Paxton *et al* since preliminary experiments determined that a larger volume of gel/cell material was required to surround the TiS during formation of the TEL[12–14,22]. The constructs were incubated at 37°C for 3 days and then fed with fresh SDMEM every 2 days for a total of 4 weeks. From day 7 onwards, the SDMEM was supplemented with 50μM proline (P0380, Sigma-Aldrich, Dorset, UK) and 250μM ascorbic acid (49752, Sigma-Aldrich, Dorset, UK).

2.4 Evaluation of mechanical properties

Initially, the mechanical properties of the TiSs with various gap sizes were investigated using an environmental Instron micro tester (model 5848, Instron, High Wycombe, UK) using a 1 kN loading cell. The spring was extended at a speed of 1 mm/min, and load-extension (L-E) values were recorded. Figure S2 (Supplementary Information Section 2.4.1) shows a schematic drawing of an L-E curve of an elastic spring. This curve can be divided into two parts: a linear part representing an elastic deformation, and a subsequent non-linear part where the spring loses its elasticity and deforms inelastically. The spring constant, k, of the

spring was calculated from the gradient linear region of the L-E graph. To test the fatigue and viscoelastic properties of the spring, a cyclic test was designed based on a deformation-controlled tensile test. The spring was extended at a speed of 1 mm/min until the deformation reached 0.5 mm, and then the load was removed at the same speed until the spring returned to its original length. This cycle was repeated 10 times, before the spring was extended again to 0.5 mm and held for 3 min.

A custom-built clamp made of aluminium alloy was used to test the physical properties of the TELs and TiS-TELs in a PBS environment at 37°C using an Instron Microtester, as shown in Supplementary Information Section S2.4.2 Figure S3. The tensile properties of the TEL were assessed at 0.4 mm/sec. The viscoelastic and fatigue properties were investigated through the same cyclic deformation.

2.5 Cell and extracellular matrix imaging
2.5.1 DAPI cell nuclear staining.

The TELs were washed in sterile phosphate buffered saline (PBS) three times, then fixed in 4% formaldehyde overnight. The specimens were then rinsed in DAPI (2 μl in 50 ml PBS) at 37°C for 3 to 5 min and finally washed in PBS. The samples was then imaged using a confocal scanning laser microscope (Leica TCS SP2, Leica Microsystems UK Ltd., Milton Keynes, UK).

### 2.5.2 Polarised light microscopy for visualising collagen alignment.

The samples with the implants were fixed in 2.5% glutaraldehyde in 0.1M sodium cacodylate buffer, pH 7.2. The samples were then transferred to 70% ethanol and cut and ground into sections, as described by Donath *et al.*[23,24], using an Exakt sawing machine and grinding equipment (Exakt Apparatebau, Norderstedt, Germany). Briefly, the samples were rinsed in water, dehydrated in ethanol (from 70% to 99%), pre-infiltrated in diluted resin and finally infiltrated and embedded in pure resin (Technovit 7200, VLC, Kulzer, Wehrheim, Germany) and polymerized in UV-light. The cured block was divided with a diamond-coated band saw. The sample surface was ground plan-parallel and glued to a plexiglass that served as the supporting object glass. An initial thick section of about 150μm was prepared and further ground in an automatic grinder using SiC water-grinding. The final surface finish was prepared with smooth-papers (2400- and 4000 grit). The sections were histologically stained in toluidine blue mixed with pyronin G, dried and mounted. Light microscopic investigations were done on the 10μm thin sections using various objectives. The collagen structures were observed with the aid of a polarising filter, with an additional lambda filter in the light source. Images were acquired with a Nikon DS-Ri camera connected to the light microscope (Nikon Eclipse ME 600L, Tokyo, Japan).

3 Results and Discussion

3.1 Cellular adhesion to titanium reinforcements and collagen arrangement

Observation of the contraction of the fibrin matrix over 4 weeks (Figure 1a) revealed that, qualitatively, the fibrin matrix of both
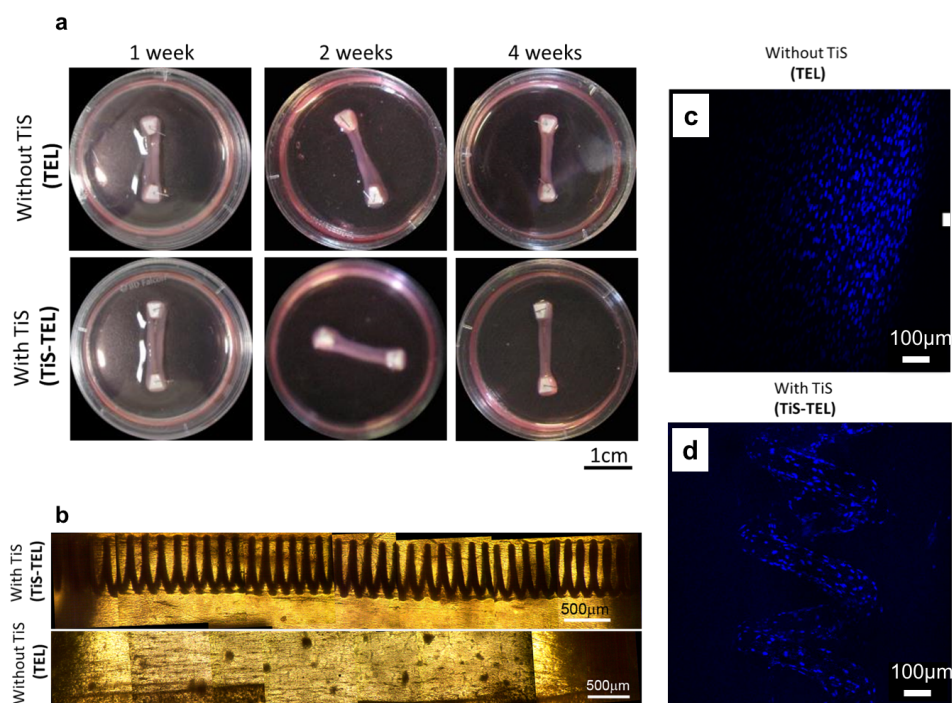
Fig. 1 Photographs of tissue-engineered ligaments (TEL) over 4 weeks in culture (a) without (top row) and with (bottom row) Titanium spring (TiS) reinforcement through the core of the tissue. The spring did not appear to inhibit cell-mediated contraction of the fibrin matrix and resulted in the formation of the typical band-like structure. (b) shows how the springs are integrated into the tissue between the brushite anchors. The confocal fluorescence images (c) and (d) show DAPI stained cell nuclei within longitudinal cross-sections of non-reinforced and reinforced constructs, respectively. The proportion of the cell population nearest to the Ti spring appeared to align with the coiling of the spring.

titanium spring reinforced tissue engineered ligaments (TiS-TEL) and non-reinforced tissue engineered ligaments (TEL) contracted form band structures of similar lateral dimensions over 1, 2 and 4 weeks. No obvious fibrin matrix misfolding, tearing or aggregation was found in the transmission light microscopy images of the constructs, as shown in Figure 1b. DAPI staining and confocal fluorescence imaging of the cell population revealed their homogenous distribution throughout the non-reinforced ligament (Figure 1c), while careful examination of the cells near the core of the TiS-TEL revealed their alignment about the coiling of the spring itself (Figure 1d). Not only does this imply that the incorporation of the spring did not inhibit cell-mediated contraction of the fibrin matrix at the centimetre 3D tissue scale, but also that intimate contact and been established between the cell seeded fibrin matrix and the length of the spring.

Examination of the surface of the Ti springs by SEM revealed a roughened and grooved surface, which may be attributed to the spring manufacturing process (Figure 2a). Chick tendon fibroblasts were cultured on to a set of Ti springs for 5 days and imaged under SEM to enable more clear visualisation of the cell-substrate contact compared to analysing a tissue section with many cell layers (Figure 2a). By day 5 the cells had reached near confluency and had adhered to and aligned along the coiling surface of the spring as indicated by the clear presence of focal adhesions in Figure 2b and c marked with white arrows. The binding affinity of the cells for the titanium surface was more clearly demonstrated in a repeat experiment using a spring with a more acute coil pitch, resulting in contact between the coils when the spring was at rest (Figure 2d). At higher magnification, some cells were observed to form focal adhesions across two adjacent coils with the main cell body suspended over the interstitial space between the coils (Figure 2e).

Cells and collagen fibres were observed to align parallel to the coils in the vicinity of the spring in Figure 3a (and shown more clearly in magnified images b, c and d), while the collagen fibres and cells found within the brown peripheral covering at the edge of the ligament (shown by the arrows in Figure 3a) were parallel to the long axis, corresponding to previous observations for the reinforced and unreinforced ligaments.
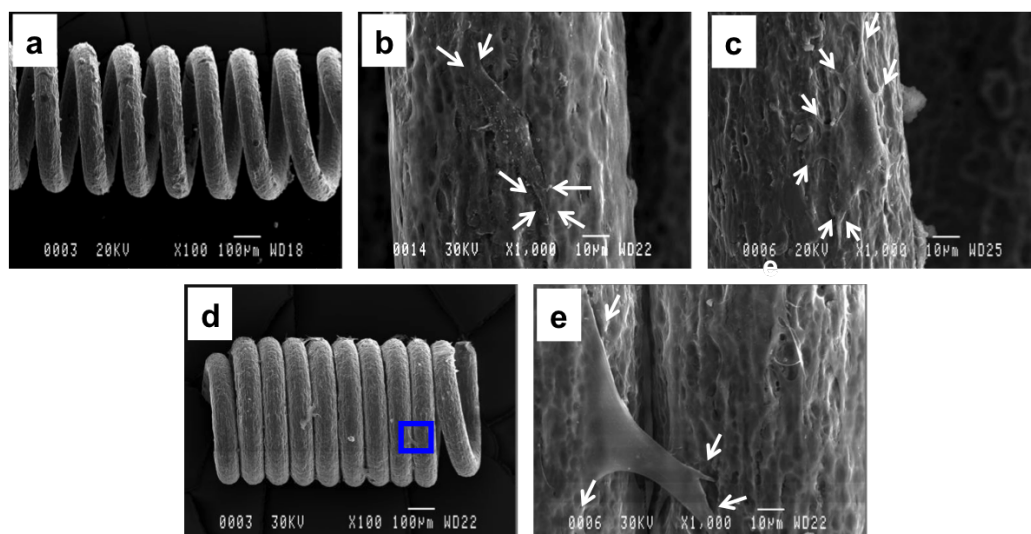
Fig. 2 Scanning Electron Microscopy (SEM) images of the same type of Titanium spring used in the Ti spring reinforced tissue engineered ligaments (TiS-TEL) cultured with chick tendon fibroblasts (CTF) for 5 days to enable clear visualisation of the nature of the cell contact with the surface of the spring (a). The cells formed a monolayer of the spring, but close inspection of higher magnification images of one of the coils revealed the presence of focal adhesions (white arrows) from cells located on the at the very top of the surface. A repeat experiment using a spring with a more acute coil pitch, to the point where the coils were in contact when under zero strain (d), demonstrated the ability of the cells to form strong adhesions as shown in (e) where a cell formed focal adhesions spanning across two coils.
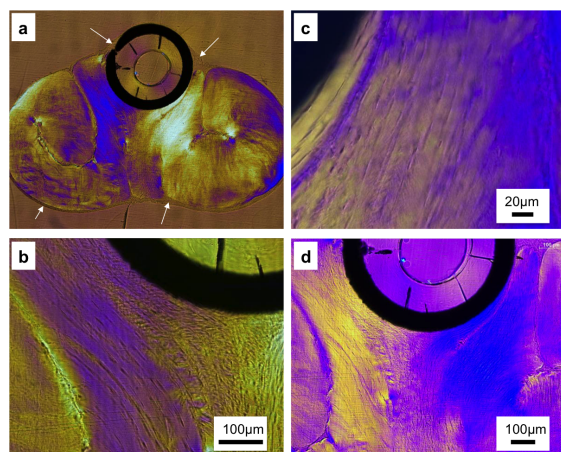
Fig. 3 Section through ligament and spring viewed by polarised light microscopy (x10). Colours are due to birefringence of collagen: the fibres adjacent to the spring curve around it (shown more clearly below) whilst the ones in the central region lie perpendicular to the long axis of the ligament. The white arrows show the residual fibrin matrix against the spring and the edge of the collagenous matrix of the construct. Higher magnification images (b, c and d below) show the alignment of the fibres more clearly.

## 3.2 Mechanical properties of reinforced constructs

3.2.1 Single extension cycle to failure

The results of a tensile test of an unreinforced tissue engineered ligament are shown in the still images from a video clip of the test Figure 4a and the stress-strain plot below (blue line). The ligament failed in two general stages with the initial linear extension phase coming to an end at a load of 510mN, giving way to a hyperextension phase under little increase in mechanical stress before complete failure at a maximum load of 720mN. Failure

of the construct occurred near the cement-construct interface, as shown in the photographs taken during mechanical testing. Fragments of brushite cement were seen on the soft tissue, indicating a high degree of adherence at the interface.

For the construct reinforced with a titanium spring, the images from the video shown in Figure 4b show that the construct mainly failed in the soft tissue region well away from the anchor as evidenced by the tissue fragments remaining on the top anchor. The stress-strain plot (orange line) shows numerous partial failures in the structure over the strain range (labelled as 2 to 10 on the plot) with much higher peak stress values compared to the unreinforced construct. This represents a far more progressive failure of the construct where partial failures occur to dissipate energy as a means of preserving the overall structure. The progressive nature of this failure in the reinforced constructs together with the complete failure occurring in the soft tissue region rather than at the hard-soft interface is significant as it mimics the failure mechanism of native ligament tissue. The spring was not pulled out of the cement until the soft tissue failed completely, with the spring undergoing plastic deformation and bearing the load. Therefore the presence of the Ti spring does not compromise the hard-soft interface by acting as a mechanical weak point.

Typical load-extension (L-E) and stress-strain (S-S) curves of TEL, TiS-TEL and TiS are shown in Figure 5. The failure mechanism of TEL and TiS-TEL differs. TEL is deformed elastically until the yielding point followed by an abrupt fracture, with $\sigma_y = \sigma_U$. TiS-TEL is also deformed elastically at the beginning. After yield, the tensile test curve of TiS-TEL displayed several partial failures until the final breakdown of the soft tissue and the residual curve represents only the properties of TiS, with $\sigma_y < \sigma_U$. It is also noted that TiS-TEL is both stronger and stiffer than TiS alone. Table 1 compares the tensile properties of the unreinforced and
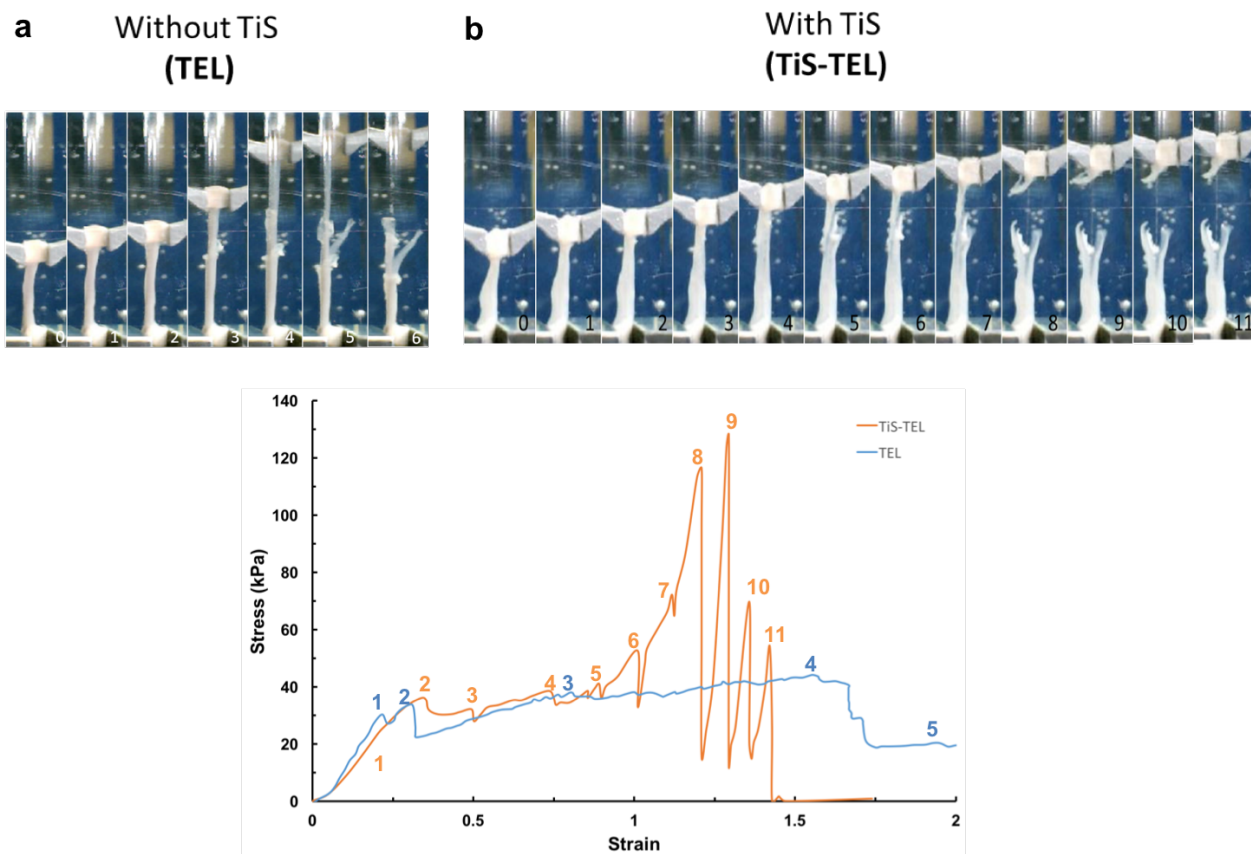
Fig. 4 Tensile mechanical testing in saline at 37°C TEL (a) and Ti-S TEL (b) to failure. Results of tensile testing of 4 week old unreinforced construct, with the load-extension curve of a titanium spring for comparison. L-E is the load-extension curve (experiment) while S-S is the derived stress-strain relationship. Stills from a video showing TEL rupture during tensile stretching. Each image corresponds to a time point labeled on the mechanical data plots below.
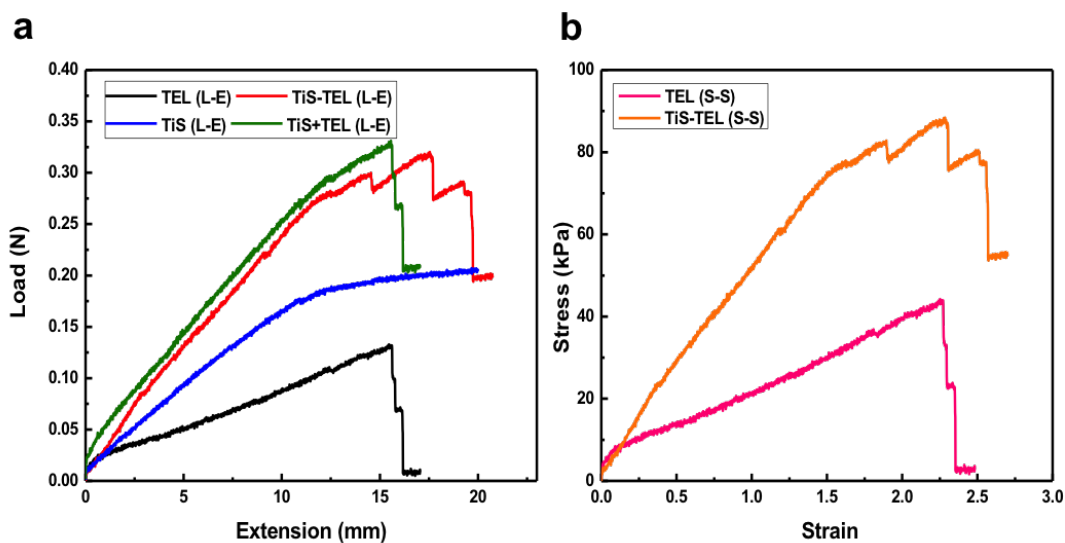
Fig. 5 Typical tensile load-extension and stress-strain curves of tissue engineered ligaments with (TiS-TEL) and without (TEL) Titanium spring reinforcement. Loading speed is 0.1 mm/s.

Table 1 properties of unreinforced tissue engineered ligament and reinforced hybrid ligament (n=5) after 4 weeks of culture. ** indicates statistical significance, p<0.05 (Student's t-test).

| Mechanical property / Sample	TEL	TiS-TEL
Stress at end of elastic behaviour (σ_y) (kPa)	43.30 ±9.96	80.14 ±28.3 **
Strain at end of elastic behaviour (ε_y)	1.97 ±0.30	1.21 ±0.17**
Ultimate tensile stress (σ_{UTS}) (kPa)	43.40 ±10.11	96.46 ±33.11 **
Ultimate tensile strain (ε_{UTS})	2.45 ±0.31	2.18 ±0.29 **
Tensile Modulus (kPa)	20.37 ±4.24	62.86 ±21.86 **
Strain energy to yield U_y (kJ/mm^3)	47.22 ±14.10	55.37 ±23.02
Strain energy to failure U_f (kJ/mm^3)	63.93 ±17.44	134.85 ±49.36 **

reinforced constructs after 4 weeks of maturation *in vitro*. The data from which these properties are derived is shown in Figure 5. The presence of the reinforcing spring doubled the stress at the elastic limit and the ultimate tensile stress and tripled the tensile modulus. Although the strain energy to failure was not significantly altered, the strain energy to yield at the end of the elastic behaviour was doubled. It was observed that where the unreinforced ligaments failed abruptly after the elastic limit, the reinforced ligaments displayed a progressive failure behaviour, with several partial failures before complete tearing of the structure.

3.2.2 Hysteresis and viscoelastic effects in cyclic load.

Stress-strain curves for cyclic loading of the reinforced and unreinforced ligament construct are displayed in Figure 6. In the case of the unreinforced ligament, the construct displays a degree of stress relaxation, as can be seen from the reduction in the peak value of stress (upper curve) and the increasing width of the plateau at the bottom of each cycle. The reinforced ligament has a much higher and more consistent peak stress, with a much lower rate of stress relaxation and no plateau at the bottom of the load cycles. No significant changes in mechanical stress or stain were found at common phases across the loading cycles until tested to failure. This suggests that the Ti spring and soft tissue largely remained bonded together and performed as a single mechanical structure until deliberately loaded to failure. When extended far beyond the elastic limit and towards complete failure, it is reasonable to assume that some degree disconnection of the tissue from the Ti spring will take place.

Analysis of the effect of cyclic loading (Figure 7) showed that there was marked hysteresis in the behaviour of both reinforced and unreinforced constructs for all cyclic strain magnitudes, but was less obvious in the reinforced constructs. The reduced degree of hysteresis in the reinforced constructs can be attributed to the elastic behaviour of the spring in conjunction with the viscoelastic behaviour of the soft tissue envelope. It was also found that cyclic pre-loading reduced the stress at which the elastic limit was reached, an effect also observed in mammalian soft tissues. The stress values at fixed strain (σ_{10}, σ_{20} and σ_{50}) are significantly decreased after the first cycle for both TEL and TiS-TEL. The maximum stress (σ_{100}) shown in each cycle was also reduced

during the cyclic test, but tends to stay stable after a few cycles. TEL becomes stiffer during the first several cyclic stretching, with a slightly increased elastic modulus (E); this tendency is weakened after the first 2 to 3 cycles and E stays stable afterwards. Compared with TEL, the modulus of TiS-TEL is stable throughout the 10 cycles. TiS-TEL has higher σ_{10}, σ_{20}, σ_{50}, σ_{100} E and u_c values than TEL, however they demonstrate similar u_c values (the overall energy required to complete each cycle). The data in Figure 7h shows normalised σ_{50} values of TEL and TiS-TEL, demonstrating the deviation of σ_{50} away from its maximum value (σ_{50} in cycle 1) during the cyclic deformation. This figure suggests that TiS-TEL is more stable during the test. Normalised σ_{10}, σ_{20}, σ_{50}, σ_{100}, E and u values follow the same tendency.
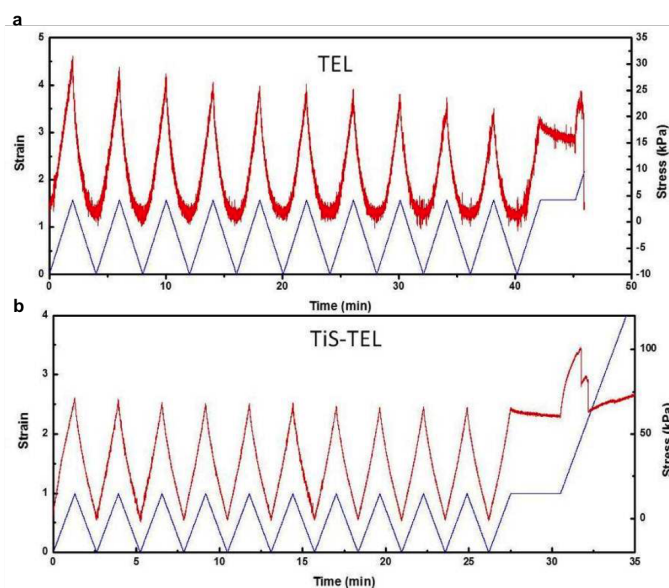
Fig. 6 Stress and Strain in the tissue engineered ligament (unreinforced - TEL, reinforced -TiS-TEL) plotted against time for the cyclic loading test. The samples were loaded at a rate of 0.1mm/s to a strain corresponding to 80% of the yield strain, for 10 cycles. The samples were then held at this extension for 3 minutes before being stretched to failure.
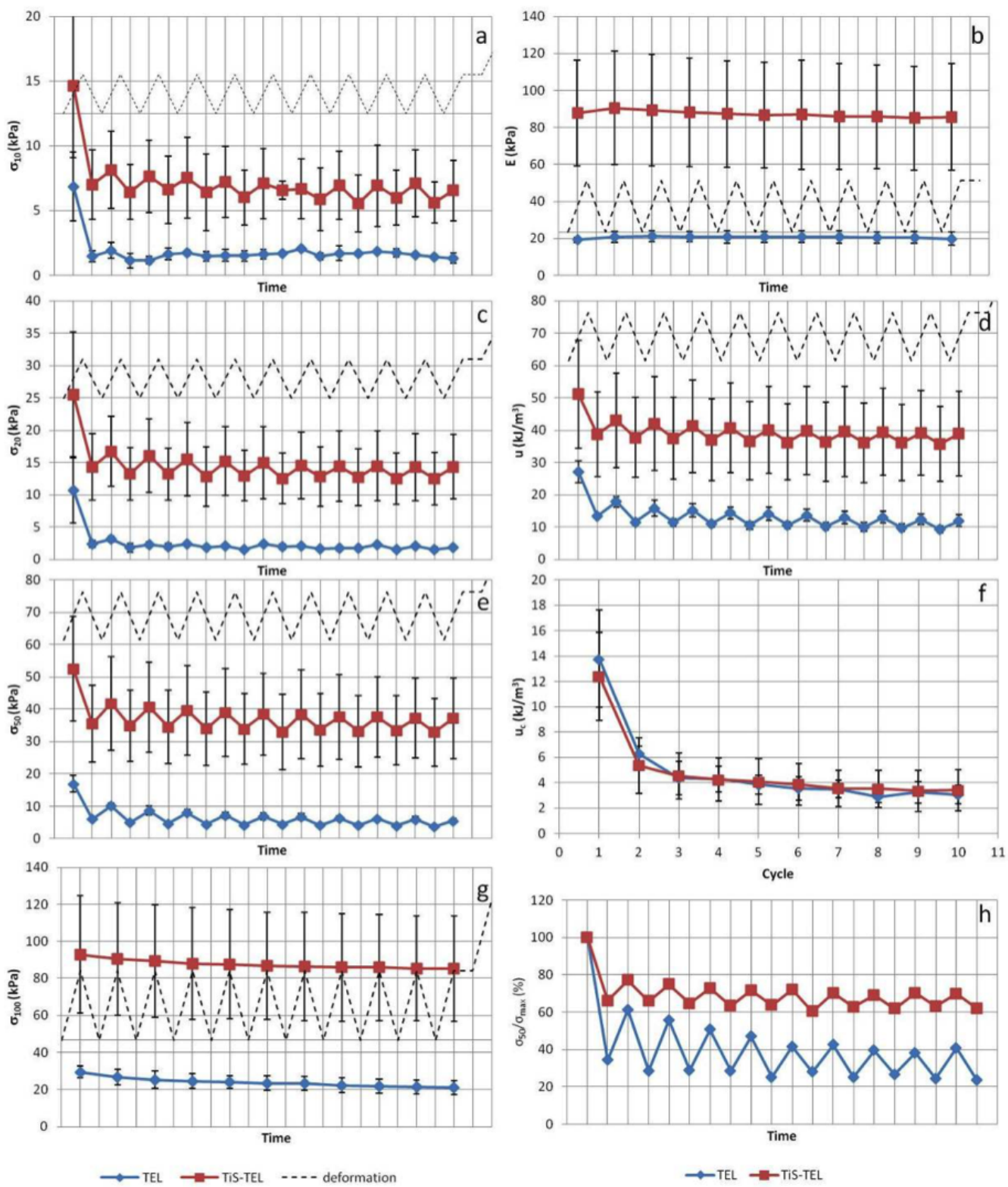
Fig. 7 Average stress values at fixed strain (σ_x), elastic modulus (E) and strain energy (u) of TEL and TiS-TEL during independent cyclic testing.

4 Conclusions

We have systematically evaluated how the spring reinforcements are integrated with the tissue from the cellular and macroscopic levels and mapped these observations to the bulk mechanical properties and dynamic loading response of the fully developed construct. Ti springs are an excellent choice of reinforcing structure because they exhibit elastic properties at length extensions in excess of those normally associated with ligaments, while the Ti material itself is known to facilitate cell adhesion when used in bone replacement implants. The incorporation of a Ti spring does not hinder contraction of the fibrin gel during manufacture of the TEL. Some evidence suggests the spring acts as third anchor point during contraction resulting in thinner TELs (smaller cross-sectional area), but this alone does not appear to compromise their mechanical integrity.

The nature of the contact between the Ti spring and the forming tissue is intimate and spans both the cellular and tissue/cell matrix level on the order of 100's of microns. Fibrin sheets containing multilayers of cells wrap around the spring with the cells generally aligned along the direction of the TEL. Cells in layers approaching the surface of the spring gradually rotate in alignment until individual cells in contact with the spring then align along the coiling direction of the spring. Collagen fibre alignment was found to mimic this pattern. This hierarchical structuring at both the cellular and tissue level provides the structural basis for improved load transmission across the TEL.

In the unreinforced TEL, failure occurs partly at the hard-soft tissue interface and partly within the soft tissue structure. In latter part, failure occurs through sequential breaking of tissue strands which make up the TEL. Spring reinforcement results in stronger, stiffer TELs with more consistent stress at fixed strain values over prolonged periods of cyclic testing. Partial failure in reinforced TELs only occurs at strains approaching total failure suggesting that the Ti springs facilitate better load distribution across the soft tissue leading up to this point, also shown by much higher consistency in testing results. Hysteresis and viscoelastic effects are considerably reduced in reinforced construct and results show that load sharing between spring and cell/scaffold construct minimises the effect of local defects and reduces tear propagation. Incorporation of the Ti spring enhances load distribution and reduces effect of stress concentrations. Therefore, our hybrid tissue engineered/synthetic ligament replacement approach shows promise with enhanced strength compared to unreinforced construct while utilising an already proven biocompatible material in musculoskeletal applications.

5 Acknowledgements

References

1 R. A. Clayton and C. M. Court-Brown, *Injury*, 2008, **39**, 1338–1344.

2 S. M. Gianotti, S. W. Marshall, P. A. Hume and L. Bunt, *Journal of Science and Medicine in Sport*, 2009, **12**, 622–627.

3 S. P. Ho, M. P. Kurylo, T. K. Fong, S. S. Lee, H. D. Wagner, M. I. Ryder and G. W. Marshall, *Biomaterials*, 2010, **31**, 6635–6646.

4 J. Kartus, T. Movin and J. Karlsson, *Arthroscopy: The Journal of Arthroscopic & Related Surgery*, 2001, **17**, 971–980.

5 J. Kartus, S. Stener, S. Lindahl, B. Engström, B. I. Eriksson and J. Karlsson, *Knee Surgery, Sports Traumatology, Arthroscopy*, 1997, **5**, 222–228.

6 S. Thomopoulos, G. M. Genin and L. M. Galatz, *Journal of musculoskeletal & neuronal interactions*, 2010, **10**, 35.

7 M. V. Hogan, Y. Kawakami, C. D. Murawski and F. H. Fu, *Arthroscopy: The Journal of Arthroscopic & Related Surgery*, 2015, **31**, 971–979.

8 L. M. Batty, C. J. Norsworthy, N. J. Lash, J. Wasiak, A. K. Richmond and J. A. Feller, *Arthroscopy: The Journal of Arthroscopic & Related Surgery*, 2015, **31**, 957–968.

9 C. Vaquette, C. Kahn, C. Frochot, C. Nouvel, J.-L. Six, N. De Isla, L.-H. Luo, J. Cooper-White, R. Rahouadj and X. Wang, *Journal of Biomedical Materials Research Part A*, 2010, **94**, 1270–1282.

10 C. K. Kuo, J. E. Marturano and R. S. Tuan, *BMC Sports Science, Medicine and Rehabilitation*, 2010, **2**, 1.

11 A. Tamayol, M. Akbari, N. Annabi, A. Paul, A. Khademhosseini and D. Juncker, *Biotechnology advances*, 2013, **31**, 669–687.

12 J. Z. Paxton, L. M. Grover and K. Baar, *Tissue Engineering Part A*, 2010, **16**, 3515–3525.

13 J. Z. Paxton, K. Donnelly, R. P. Keatch and K. Baar, *Tissue Engineering Part A*, 2008, **15**, 1201–1209.

14 J. Z. Paxton, P. Hagerty, J. J. Andrick and K. Baar, *Tissue Engineering Part A*, 2011, **18**, 277–284.

15 K. E. Kadler, D. F. Holmes, J. A. Trotter and J. A. Chapman, *Biochemical Journal*, 1996, **316**, 1–11.

16 K. E. Kadler, C. Baldock, J. Bella and R. P. Boot-Handford, *Journal of cell science*, 2007, **120**, 1955–1958.

17 S. Englard and S. Seifter, *Annual review of nutrition*, 1986, **6**, 365–406.

18 B. Peterkofsky, *The American journal of clinical nutrition*, 1991, **54**, 1135S–1140S.

19 Z. Xia, L. M. Grover, Y. Huang, I. E. Adamopoulos, U. Gbureck, J. T. Triffitt, R. M. Shelton and J. E. Barralet, *Biomaterials*, 2006, **27**, 4557–4565.

20 L. M. Grover, U. Gbureck, A. J. Wright, M. Tremayne and J. E. Barralet, *Biomaterials*, 2006, **27**, 2178–2185.

21 L. M. Grover, A. J. Wright, U. Gbureck, A. Bolarinwa, J. Song, Y. Liu, D. F. Farrar, G. Howling, J. Rose and J. E. Barralet, *Biomaterials*, 2013, **34**, 6631–6637.

22 J. Z. Paxton, K. Donnelly, R. P. Keatch, K. Baar and L. M. Grover, *Annals of biomedical engineering*, 2010, **38**, 2155–2166.

23 K. Donath and G. Breuner, *Journal of Oral Pathology & Medicine*, 1982, **11**, 318–326.

24 K. Donath, *Norderstedt: Exakt-kulzer-publication*, 1993, 1–16.